Polymer Testing 41 (2015) 149–156

Contents lists available at ScienceDirect

Polymer Testing

journal homepage: www.elsevier.com/locate/polytest

Property modelling

Prediction of the morphology of polymer-clay nanocomposites

M. Ceraulo [a], M. Morreale [b], L. Botta [a], M.C. Mistretta [a], R. Scaffaro [a, *]

[a] Università di Palermo, Dipartimento di Ingegneria Civile, Ambientale, Aerospaziale, dei Materiali, Viale delle Scienze, 90128 Palermo, Italy
[b] Università degli Studi di Enna "Kore", Facoltà di Ingegneria e Architettura, Cittadella Universitaria, 94100 Enna, Italy

ARTICLE INFO

Article history:
Received 8 October 2014
Accepted 18 November 2014
Available online 25 November 2014

Keywords:
Nanocomposites
Morphology
Rheological properties
Modelling

ABSTRACT

Polymer nanocomposites have continually attracted increasing interest over the last decade, due to significant improvements they can offer compared to neat polymer matrices. However, the final morphology of a nanocomposite, determined by several variables, can significantly influence the macroscopic properties of the final product. Therefore, it is important to study the interactions between processing, morphology, structure and rheological properties, and the suitability of existing models in order to predict the system's behaviour with change of the main processing variables.

In this work, the applicability of a predictive theory based on the Wu model was formulated and proposed in order to predict the morphology of nanocomposite systems. This theory allows description of a polymer matrix - lamellar filler system, provided that the interactions between the two components and the processing are known. In particular, a lamellar filler has been considered as a deformable second component of a blend, with its behaviour depending on the processing and on the interactions with the polymer matrix. This allowed analyzing different behaviour for the systems, due to the different polarity of the matrix, which may lead to a classification of polymer nanocomposites in two or more families, according to their different matrix polarities.

1. Introduction

Polymer nanocomposites have attracted great interest over the last decade [1,2]. It is known [2–4] that the use of nanometric fillers dispersed in polymer matrices can result in significant improvements in comparison with the neat polymer matrices, such as the enhancement of elastic modulus and tensile strength, as well as thermal, electrical and barrier properties of the systems. All these improvements can be achieved even with filler amounts as low as 5 wt% [3,4]. In addition, polymer nanocomposites, are attracting increasing interest beyond the academic and scientific field in industry [2,4].

The final morphology of a nanocomposite (determined by several variables such as the processing parameters, the matrix and nanofiller used, their mutual interactions, etc.) significantly influences the macroscopic properties of the final product [5–7]. In particular, it becomes central to learn about the interactions between processing, morphology, structure and rheological properties, and the suitability of existing models in order to predict the system's behaviour with change of variables such as the polymer used, filler content and processing speed.

Among the various nanometric fillers which have been used in combination with thermoplastic matrices, the most widely investigated are clays [6,7]. Thermoplastic-clay

* Corresponding author.
E-mail address: roberto.scaffaro@unipa.it (R. Scaffaro).

http://dx.doi.org/10.1016/j.polymertesting.2014.11.005
0142-9418/

polymer nanocomposites can show different mechanical, rheological and morphological properties depending on the matrix used, filler content, their mutual interactions and processing techniques, as well as reprocessing [8–10].

A possible way of understanding the relative interactions between those variables is to apply the Wu model [11], usually adopted to describe the behaviour of polymer blends.

The aim of this work is, therefore, to investigate the applicability of the Wu model in order to predict the morphology of the nanocomposite. In particular, the possible applicability and limits of this existing model by changing some conditions such as polymer matrix type, filler content and processing conditions was assessed. The Wu model, usually applied to polymer blends, was here used for the prediction of the morphology of thermoplastic based nanocomposites considering the clay as a deformable phase [12].

In particular, different combinations between an organically modified clay and polymer matrices with different polarity have been investigated.

2. Theoretical background

Studies on polymer blend models are usually based on determining some parameters of the investigated systems such as, for instance, the viscosity of the dispersed phase. In the present work, according to previous findings, it was assumed that the clay, dispersed in the matrix, is a deformable phase [12,13]. For this nanofiller, it is very difficult to determine the rheological behaviour since it is not possible to measure an actual viscosity, but rather a parameter that takes into account its plasticity/deformability under flow. In particular, this parameter should be able to give quantitative information regarding the capability of the tactoid platelets to mutually slide when subjected to a shear stress up to separation and, eventually, dispersal in the matrix, in the same way as a second polymer component in a blend would do. Since it is clearly impossible to obtain such measurements experimentally, the Wu model [11], which is valid for polymer blends, was used: the clay was thus considered as the second deformable component of a polymer blend.

Therefore, after preparing the nanocomposites, the parameters for the Wu equation were determined. The Wu model is described by Eqn. 1:

$$D = \left(\frac{4\sigma \cdot \lambda^{0.84}}{\eta_m \dot{\gamma}}\right) \quad (1)$$

Or, equivalently,

$$\lambda = (\dot{\gamma}\eta_m D/4\sigma)^{1/0.84} \quad (2)$$

where D is the average equivalent diameter of the dispersed phase, σ is the clay-polymer interface tension, η_m is the polymer matrix viscosity, $\dot{\gamma}$ is the shear rate, λ is the ratio between viscosity of the dispersed phase, η_d, and the viscosity of the matrix, η_m: $\lambda = \eta_d/\eta_m$.

As regards the determination of the equivalent diameter, the following procedure was performed.

First, the length and width (major and minor axes of each particle, considered as an ellipse) of at least one hundred particles was measured on several SEM micrographs and their areas, A_i, were calculated.

Then, a probability plot of A_i-s was created for each system. This allowed determining the average area, A_{eq}, from which the average equivalent diameter, D_{eq}, was calculated according to Equation 3:

$$D_{eq} = \left(4A_{eq}/\pi\right)^{1/2} \quad (3)$$

Furthermore, the possible presence of an applicability limit, due to phenomena not taken into account by the Wu model (such as, for instance, coalescence), was investigated. This limit might be, for instance, an upper limit of concentration, i.e. when the filler percent is too high, the relative hypothesis of independence of the particles of the dispersed phase is not valid anymore due to coalescence.

3. Materials and methods

3.1. Materials

The polymers used in this work were a polyamide-6 (PA6), produced by Radicinova Spa (Italy) with the commercial name “Radilon S35 NAT” (intrinsic viscosity in sulphuric acid: 3.4 dl/g) and a high density polyethylene (HDPE) supplied by Polimeri Europa (Italy) as “Eraclene MP94” (density = 0,96 g/cm^3, melt flow index = 7g/10 min at 2.16 kg load). The lamellar nanofiller was an organo-modified clay sample, Cloisite® 15A (Southern Clay Products, USA). Cloisite 15A (CL15A) is a ditallowdimethylammonium modified montmorillonite, with an average diameter of 8 μm; the organo - modifier concentration is 125 meq/100 g clay.

The polyamide was dried in a ventilated oven at 90 °C for 10 h and then in a vacuum oven at 120 °C prior to processing, in order to prevent hydrolytic chain scission during processing.

3.2. Preparation

The systems were prepared by using a Brabender (Germany) PLE 330 batch mixer at different speed (32, 50, 60, 100 rpm). The operating temperature was set at 190 °C for the HDPE-based systems, whereas 240 °C was chosen for the PA6-based ones. Filler content was chosen to be 1 wt%, although higher percentages (up to 10 wt%) were also taken in to account for comparison purposes.

3.3. Characterization

The specimens for characterization were obtained by compression molding using a laboratory press (Carver, USA), operating at the same temperatures adopted for processing.

Morphology of the samples was investigated using a FEI (USA) Quanta 200F scanning electron microscope (SEM) on samples broken in liquid nitrogen and covered with gold to avoid electrostatic discharge during the measurement.

The interface tension was determined according to the method proposed by Lewin et al. [14]. In particular, the clay-polymer interface tension, $\sigma_{1,2}$, can be calculated starting from the values of the surface tension of both polymer, σ_1, and clay, σ_2, as reported in Eqn. 4:

$$(\sigma_{1,2})^{1/2} = \left(\sigma_1^{1/2} - \sigma_2^{1/2}\right)^2 \quad (4)$$

The same method was adopted to evaluate the surface tension of Cloisite 15A using water as dropping fluid.

The surface tension of the neat polymer was determined by using the hanging drop method [15] and that of the clay according to a procedure proposed by Neumann [16]. This method allows calculating the surface tension of a solid by using a liquid with known surface tension, and by measuring the contact angle between this liquid and the solid under investigation, according to Eqn. 5:

$$\cos\theta_L = 2(\gamma_S/\gamma_L)^{0.5} \exp\left[-\beta(\gamma_L - \gamma_S)^2\right] - 1 \quad (5)$$

where: $\beta = 0.0001247$, γ_S is the surface tension of the solid, and γ_L is the surface tension of the liquid. As previously stated, the chosen liquid was water, with known surface tension (72.5 mJ/m^2). Contact angle between water and clay was then measured, and this allowed calculating the surface tension of Cloisite 15A. Finally, by using Eqn. 4, polymer-clay interface tension was obtained.

Contact angle measurements were carried out using a First Ten Angstrom (USA) FTA1000C apparatus, in order to determine surface tension of the neat, molten polymers. This apparatus is equipped with a heated chamber, which was set at 190 °C when analyzing the HDPE and 240 °C when analyzing the PA6. Surface tension of the molten polymers was thus measured by performing the calculation on a single drop of molten polymer hanging from a capillary inside the heated chamber and formed one hour after introducing a polymer filament into the chamber itself.

The contact angle between clay and water was determined by using the same apparatus; this measurement being necessary in order to calculate clay surface tension. The measurement was performed on clay tablets obtained by using a laboratory tableting machine. The contact angle between the tablet and a water drop was then measured.

The shear rate, $\dot{\gamma}$, was calculated according to the model proposed by Marquez et al. [17]. This model takes into account several factors, such as shape parameters of the processing apparatus (in the present case the batch mixer), as well as parameters which depend on the processed

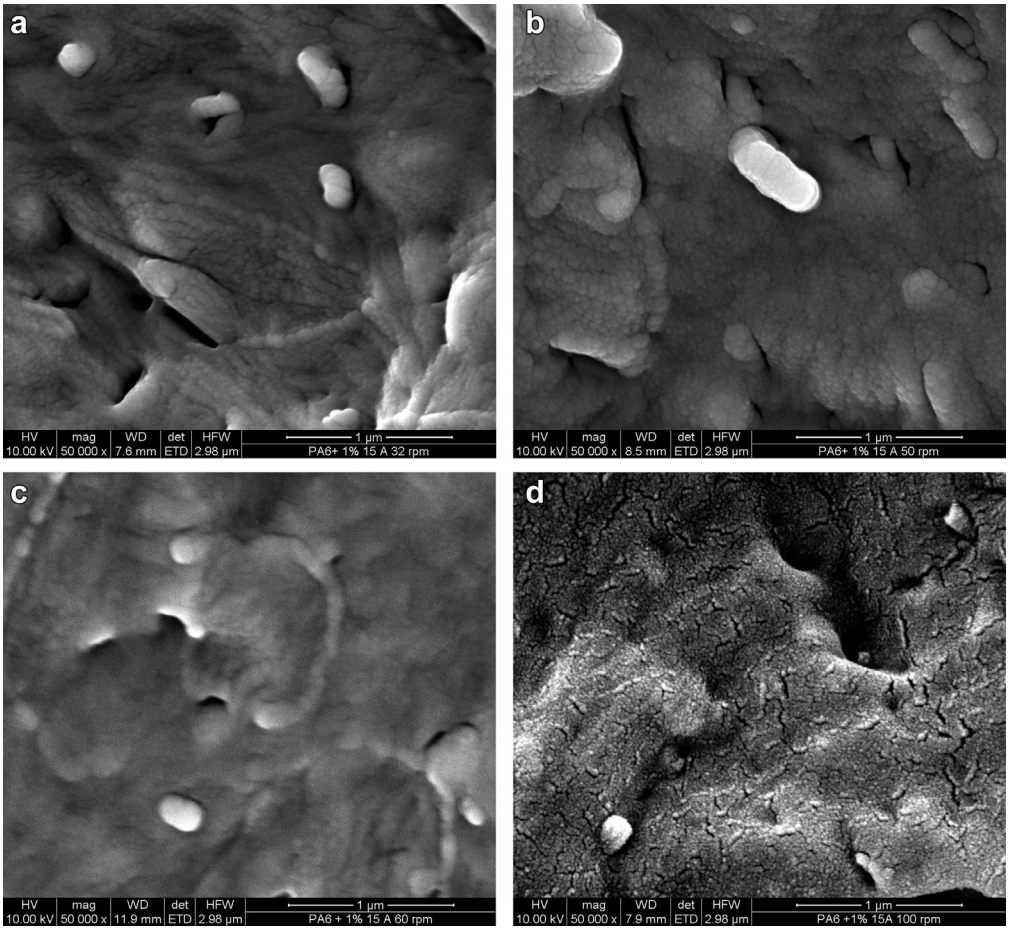

Fig. 1. a–d – PA6 + 1% cloisite 15A (a) 32 rpm, (b) 50 rpm, (c) 60 rpm, (d) 100 rpm.

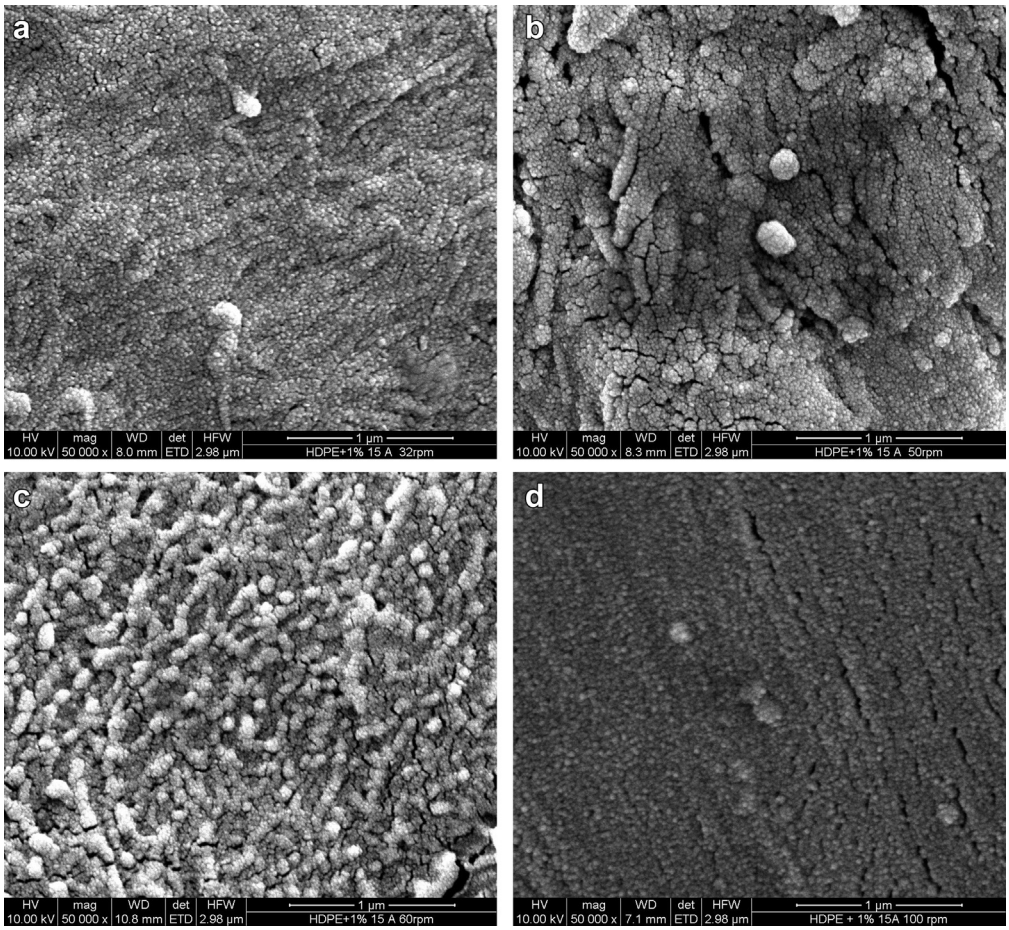

Fig. 2. a–d – HDPE + 1% Cloisite 15A (a) 32 rpm, (b) 50 rpm, (c) 60 rpm, (d) 100 rpm.

Table 1
Average equivalent diameters.

Material	Average equivalent diameter [nm]
CL 15A	3464 ± 139
PA6 + 1% CL15A@32rpm	357 ± 14
PA6 + 1% CL15A@50rpm	340 ± 14
PA6 + 1% CL15A@60rpm	300 ± 12
PA6 + 1% CL15A@100rpm	253 ± 10
HDPE + 1% CL15A@32rpm	221 ± 9
HDPE + 1% CL15A@50rpm	161 ± 6
HDPE + 1% CL15A@60rpm	157 ± 6
HDPE + 1% CL15A@100rpm	135 ± 5

Table 2
Calculated shear rates.

System	Shear rate, s^{-1}
PA6 + 1% CL15A@32rpm	17.5
PA6 + 1% CL15A@50rpm	27.4
PA6 + 1% CL15A@60rpm	33.6
PA6 + 1% CL15A@100rpm	54.5
HDPE + 1% CL15A@32rpm	17.9
HDPE + 1% CL15A@50rpm	27.4
HDPE + 1% CL15A@60rpm	33
HDPE + 1% CL15A@100rpm	54.9

materials. In detail, the shear rate is calculated as a function of parameters such as the angular speed of the mixer's rotating cams, the flux index (which depends on the measured torque) and a shape parameter which depends in turn on the shape characteristic of the mixer's rotating cams.

Finally, the viscosity of the polymer matrix, η_m, was determined directly from the rheological tests performed on a Rheometric Scientific (USA) RDAII plate-plate rotational rheometer.

4. Results and discussion

4.1. Determination of the viscosity ratio

The calculation of the viscosity ratio, λ, depends on determination of all of the parameters appearing in the Wu equation, as described in the Theoretical Background section. The equivalent diameter, D, was calculated as average diameter according to the methods described above (Equation 3), using the data obtained from particle size measurements performed on the SEM micrographs.

For sake of conciseness, only some representative SEM micrographs are reported in Fig. 1 and Fig. 2.

The results obtained for the calculation of the average equivalent diameter of the various systems investigated are reported in Table 1.

It can be observed that the average diameter of CL15A is drastically reduced comparing the neat clay and the clay dispersed in the nanocomposites. As expected [7,9,10,18], the use of different matrices and different processing speed induces different particle dimensions: in HDPE smaller particles sizes are observed, if compared with PA6, while further reduction was obtained for both systems by increasing the rotational speed, and thus the shear stress [13]. At these filler contents and dispersion levels, the model is expected to be sufficiently accurate; however, reagglomeration phenomena which may occur at higher filler contents were not taken into account, since the Wu model itself does not do so.

The shear rate was obtained according to the methods described previously and the values are reported in Table 2. As expected, it significantly increases with increasing processing speed, while there is no significant difference with change of the polymer matrix.

The matrix viscosity, η_m, was directly calculated by rheological measurements performed on a parallel plate rheometer. For sake of conciseness, only some relevant example of the rheological curves are shown in Fig. 3. While PA6 shows a deviation from the Newtonian behaviour only at higher frequencies, HDPE has a clearly detectable non-Newtonian behaviour over the whole frequency range (see Fig. 3).

In order to find the surface tension of the polymers, the hanging drop method was used, as previously described: the polymer was introduced into a capillary, which was in turn introduced into the heated chamber; the latter was heated up to the processing temperature of the polymer. Fig. 4, a-d shows the modifications underwent by the polymer with time. It is worth noting that it was necessary to hold the system for several minutes in order to correctly perform the measurement.

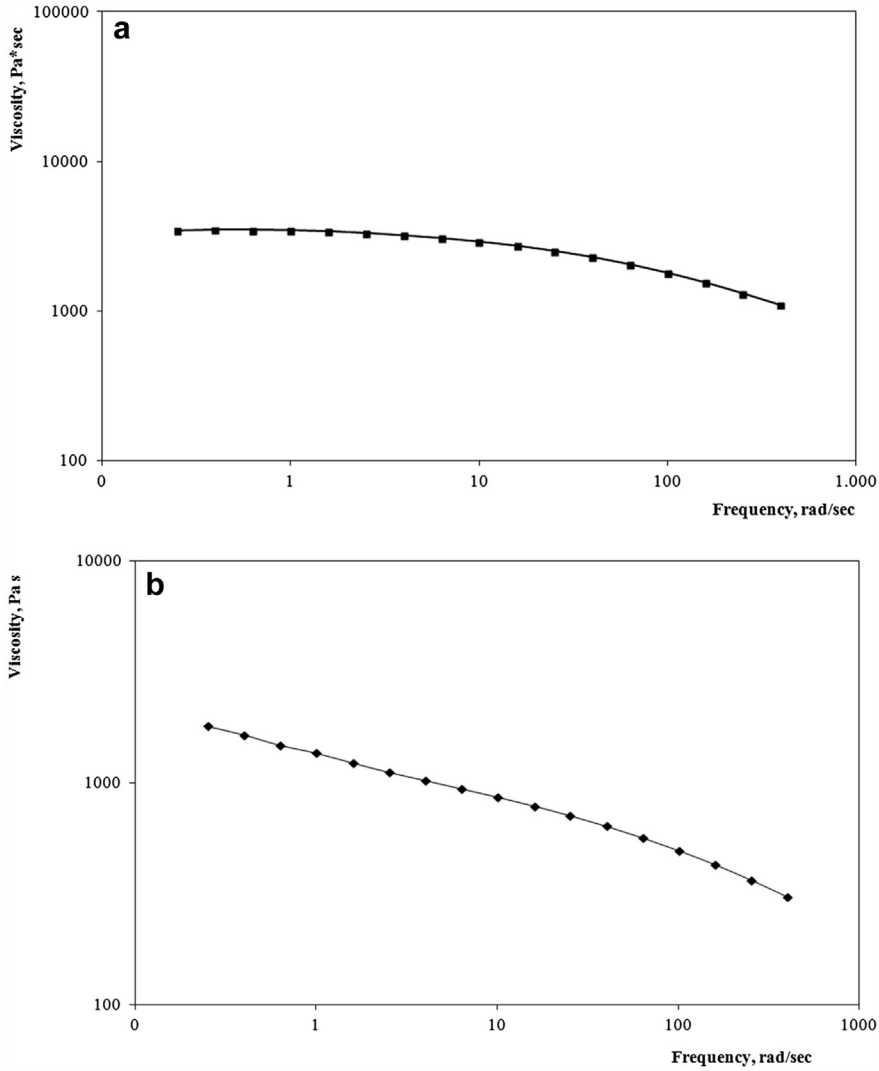

Fig. 3. a–b – Rheological curves of PA6 (a) and HDPE (b) matrices.

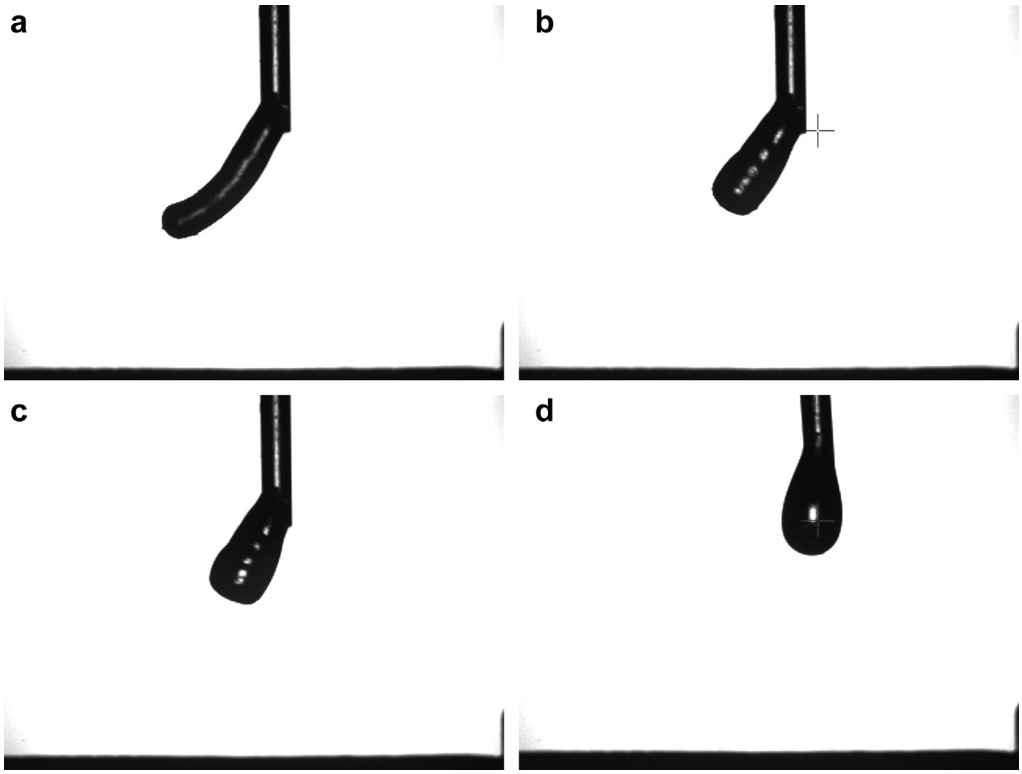

Fig. 4. a–d – Evolution of the polymer inside the heated chamber with time, from 1 min after the introduction into the chamber (a) up to 5 min (b), 10 min (c) and 20 min (d).

This allowed finding that the surface tension is 41.7 mJ/m^2 for molten PA6 and 17.6 mJ/m^2 for molten HDPE.

As regards the surface tension of Cloisite 15A, the measurements led to the determination of the contact angle between clay and water, which proved to be equal to 83°. Thus, by using the Equation (5), the calculated surface tension value of Cloisite 15A was 33.4 mJ/m^2. Subsequently, it was possible to calculate the polymer-clay interface tension in the nanocomposites from Eqn. (4). The results are reported in Table 3.

Finally, after having determined all the parameters in the Wu equation, Eqn. 1, it was possible to calculate the viscosity ratio, λ, and then, knowing η_m, the flow parameter of the dispersed phase, η_d, according to Eqn. 1. The results are shown in Tables 4 and 5.

The significantly different values found for the clay flow parameter by changing the polymer matrix revealed that the dispersed phase (i.e. the nanoclay) interacts in a very different way with the specific continuous phase (polymer matrix) where it is included.

Actually, there is a significant difference (one order of magnitude) in η_d if the matrix is HDPE or PA6. This suggests that the flow parameter of the dispersed phase, which is a lamellar silicate, is not an intrinsic property of the phase, but depends on the dispersed phase-matrix couple. On the other hand, the flow parameter of the dispersed phase seems not to depend significantly on the shear rate.

Table 3
Calculated polymer-clay interface tension values.

Polymer-clay pair	Interface tension, mJ/m^2
PA6-CL15A	0.21
HDPE-CL15A	6.2

Table 4
Calculated viscosity ratio.

System	λ
PA6 + 1%CL15A 32 rpm	51.8 ± 2.5
PA6 + 1%CL15A 50 rpm	51.2 ± 2.4
PA6 + 1%CL15A 60 rpm	52.2 ± 2.5
PA6 + 1%CL15A 100 rpm	54.7 ± 2.6
HDPE + 1%CL15A 32 rpm	4 ± 0.2
HDPE + 1%CL15A 50 rpm	4.4 ± 0.2
HDPE + 1%CL15A 60 rpm	4.2 ± 0.2
HDPE + 1%CL15A 100 rpm	5.6 ± 0.3

Table 5
Calculated flow parameter of the dispersed phase.

System	η_d [Pa s]
PA6 + 1%CL15A 32 rpm	$1.4 \pm 0.6 \times 10^5$
PA6 + 1%CL15A 50 rpm	$1.3 \pm 0.5 \times 10^5$
PA6 + 1%CL15A 60 rpm	$1.2 \pm 0.45 \times 10^5$
PA6 + 1%CL15A 100 rpm	$1.2 \pm 0.4 \times 10^5$
HDPE + 1%CL15A 32 rpm	$0.31 \pm 0.1 \times 10^4$
HDPE + 1%CL15A 50 rpm	$0.32 \pm 0.1 \times 10^4$
HDPE + 1%CL15A 60 rpm	$0.26 \pm 0.1 \times 10^4$
HDPE + 1%CL15A 100 rpm	$0.3 \pm 0.1 \times 10^4$

In order to go deeper inside this aspect, the main differences between the matrices which might influence the different interactions with the filler were taken into account. One of these could be the different polarity. Therefore, in order to assess whether Cloisite15A has different rheological behaviour depending on the polarity of the polymer matrix, this latter property was evaluated again by contact angle measurements. In particular, it was found that the contact angle between 15A and PA6 is 62° and 102° when HDPE is used instead. Therefore, PA6 is far more polar than HDPE, thus confirming that the clay behaves in a different way when the matrix has different polarity. Its flow parameter or, better, its resistance to deformation in the bulk of the matrix, depends significantly on the polarity of the matrix: the values (Table 5) are higher when it is dispersed in a more polar matrix such as PA6, while they can become even an order of magnitude lower when a less polar matrix, such as HDPE, is used.

The difference between the PA6 and HDPE based materials remains as great as one order of magnitude but, in this case, differently from the flow parameters, there is some shear rate dependency, especially for the HDPE based systems. In fact, PA6 based blends show a viscosity ratio of about 52, with a slight monotonic increase on increasing the shear rate up to a maximum value of 54.7. As regards HDPE blends, the values range from 3.6 to 5.6 with a maximum value observed when the highest shear rate is applied. It can, therefore, be concluded that there is a substantial invariance of this parameter with the shear rate.

Furthermore, other important considerations can be drawn: i) the first regards the relationship between the matrix polarity and the viscosity ratio, where the latter is clearly lower when the lower polarity matrix is adopted; ii) conversely, the more hydrophilic PA6 leads to higher viscosity ratios than those observed when HDPE was used. Therefore, it is possible to hypothesize some way of classification of nanocomposite systems based on the polarity of the matrix. This classification based on viscosity ratios can be, as pointed out previously, of significant importance since most of the theoretical models available in the scientific literature regarding the behaviour of blends take into account only the dimensions of the dispersed phase as a function of the viscosity ratio.

The second aspect regards the relationships between the viscosity ratio and the shear rate. It can be observed from the curves that the viscosity ratio is practically unchanged on increasing the shear rate, thus leading to an important consideration, i.e. the viscosity ratio does not depend on the shear rate applied.

4.2. Validation of the model

The above described model was thus validated by comparing its predictions with the experimental results obtained with changing the filler content. In particular, the possible presence of an applicability limit of the model, due to phenomena not taken into account by the Wu model (such as, for instance, coalescence) was investigated. This limit might be, for instance, an upper limit of concentration, i.e. when the filler percent is too high, the relative hypothesis of independence of the particles of dispersed phase is not valid anymore, due to coalescence.

The first filler content to be taken into account was 2 % by weight.

These systems were prepared using the same methods as for 1% filler, and filler particle dimensions were evaluated through SEM analysis as before. These were compared with the theoretical ones estimated by using the Wu model. The obtained experimental results match the theoretical ones quite satisfactorily, thus it can be concluded that the model gives a satisfactory prediction of the real experimental data.

A further investigation was, therefore, made with 5 wt% filler content. From Table 6, it can be easily observed that, even in this case, the experimental values are very close to the theoretical ones, thus confirming that the model provides a good description of the actual nanocomposites morphology under different processing parameters.

The good agreement between the theoretical and the experimental values of the diameter allows hypothesizing that the proposed model, and in particular the use of the viscosity ratio parameter where the nanofiller is considered as a deformable, dispersed phase (such as, for instance, a secondary component of a polymer blend), provides reliable information. However, when 10 wt% of filler was added, the accordance between the model and the experimental data was significantly worse, as the theoretical values were significantly different from the actual values both for HDPE and PA6. As suggested earlier, the model cannot accurately predict the actual behaviour of 10% filled systems, probably due to coalescence which is not considered by the model, but that can occur when relatively high filler percentages are present [10,18]. This can be also seen by considering Figs. 5 and 6, where the trend of

Table 6
Comparison between theoretical equivalent diameter and experimental equivalent diameter on increasing filler content.

Material	Deq [nm] theoretical	Deq [nm], experimental, 2%	Deq [nm], experimental, 5%	Deq [nm], experimental, 10%
Cloisite 15 A	3464	3464	3464	3464
PA6 + cl 15A [32 rpm]	357	357	373	210
PA6 + cl 15A [50 rpm]	340	341	340	197
PA6 + cl 15A [60 rpm]	300	301	305	192
PA6 + cl 15A [100 rpm]	253	252	253	188
HDPE + cl 15A [32 rpm]	212	212	212	214
HDPE + cl 15A [50 rpm]	197	195	198	200
HDPE + cl 15A [60 rpm]	138	141	139	198
HDPE + cl 15A [100 rpm]	135	124	124	224

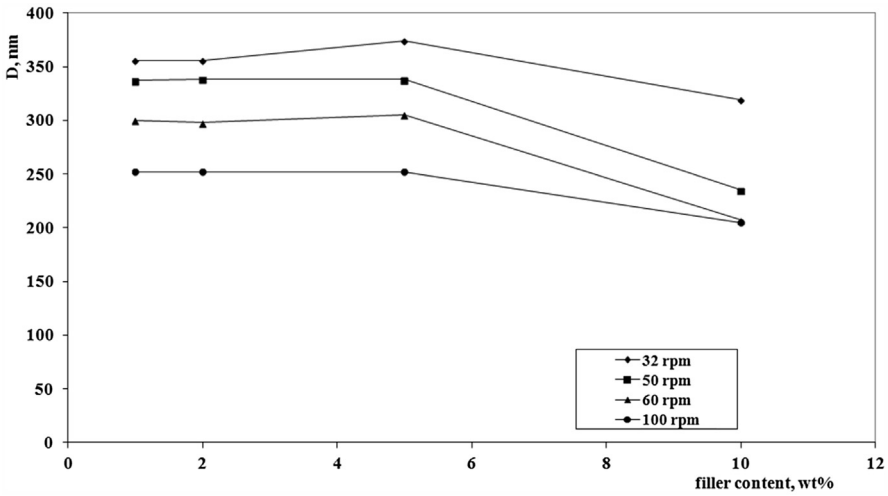

Fig. 5. D as a function of the filler content, PA6 composites.

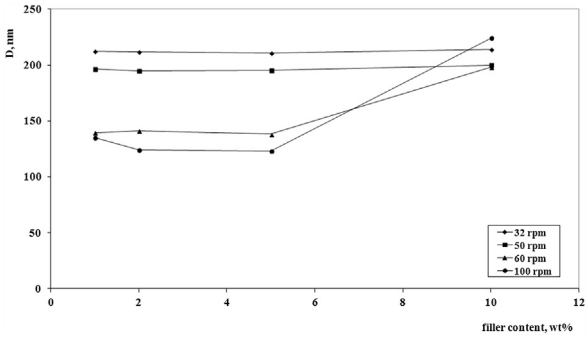

Fig. 6. D as a function of the filler content, HDPE composites.

actual D for PA6 and HDPE as a function of filler content is shown: the deviation from the theoretical value at higher filler concentrations is clearly observable.

In this respect, the coalescence phenomena can reasonably occur in HDPE systems since they show lower melt viscosities and, therefore, lower shear stress applied to the clay particles which, as a consequence, are more ready to agglomerate. Differently, in the PA6 systems, the higher viscosity of the matrix leads to higher stresses which, in turn, can reduce the dispersed phase dimensions, as typically observed in multiphasic polymer systems [19,20]. This would, therefore, lead to an actual D_{eq} lower than the theoretical, calculated one, as observed.

5. Conclusions

In this work, a predictive theory was formulated and proposed in order to correlate process parameters, morphology and rheological properties of nanocomposite systems. This theory allows describing a polymer matrix - lamellar filler system, provided that the interactions between the two components and the processing are known. In particular, the lamella filler has been considered as a deformable second component of a blend. This "deformability" of the nanoclay depends on the processing (shear rate) and on the interaction, at the chosen processing temperature, between the latter and the matrix in which it is dispersed.

References

[1] M. Alexandre, P. Dubois, Mater. Sci. Eng. 28 (2000) 1–63.
[2] G. Beyer (Ed.), Industry Guide to Nanocomposites, Applied Market Information Ltd, Bristol, UK, 2009.
[3] A. Usuki, Y. Kojima, M. Kawasumi, A. Okada, Y. Fukushima, T. Kurauchi, J. Mat. Res. 8 (1993) 1179–1184.
[4] R. Pfaendner, Polym. Degrad. Stab. 95 (2010) 369–373.
[5] N.Tz Dintcheva, R. Arrigo, M. Morreale, F.P. La Mantia, R. Matassa, E. Caponetti, Polym. Adv.Tech. 22 (2011) 1612–1619.
[6] F.P. La Mantia, M.C. Mistretta, M. Morreale, Macromol. Mat. Eng. 299 (2014) 96–103.
[7] R. Scaffaro, L. Botta, M.C. Mistretta, F.P. La Mantia, Expr. Polym. Lett. 7 (2013) 873–884.
[8] M.C. Mistretta, M. Morreale, F.P. La Mantia, Polym. Degrad. Stab. 99 (2014) 61–67.
[9] R. Scaffaro, L. Botta, M. Ceraulo, F.P. La Mantia, J. Appl. Polym. Sci. 122 (2011) 384–392.
[10] R. Scaffaro, M.C. Mistretta, F.P. La Mantia, Polym. Degrad. Stab. 93 (2008) 1267–1274.
[11] S.H. Wu, Polym. Eng. Sci. 27 (1987) 335–343.
[12] F.P. La Mantia, N.T. Dintcheva, R. Scaffaro, R. Marino, Macromol. Mat. Eng. 293 (2008) 83–91.
[13] M. Ceraulo, L. Botta, R. Scaffaro, M.C. Mistretta, F.P. La Mantia, Polym. Test. 37 (2014) 12–18.
[14] M. Lewin, A. Mey-Maron, R. Frank, Polym. Adv. Tech. 16 (2005) 429–441.
[15] D.Y. Kwok, L.K. Cheung, C.B. Park, A.W. Neumann, Polym. Eng. Sci. 38 (1998) 757–764.
[16] M. Zenkievicz, Polym. Test. 26 (2007) 14–19.
[17] A. Marquez, J. Quijano, M. Gaulin, Polym. Eng. Sci. 36 (1996) 2556–2563.
[18] F.P. La Mantia, M. Morreale, R. Scaffaro, S. Tulone, J. Appl. Polym. Sci. 127 (2013) 2544–2552.
[19] R. Scaffaro, M. Morreale, F. Mirabella, F.P. La Mantia, Macromol. Mat. Eng. 296 (2011) 141–150.
[20] M. Morreale, N. Tz Dintcheva, F.P. La Mantia, Polym. Int. 60 (2011) 1107–1116.